International Journal of Innovative Research in Engineering and Management (IJIREM)
ISSN (Online): 2350-0557, Volume 13, Issue 2, April 2026
DOI: https://doi.org/10.55524/ijirem.2026.13.2.3
Article ID IJIRE-1430, Pages 12-24
www.ijirem.org

Green Synthesis of Manganese Oxide Nanoparticles Using Plant Extracts: Synthesis Methods, Characterization, and Biomedical Applications — A Review

Ayushi Verma

Department of Life Sciences, Kalindi College, University of Delhi, New Delhi, India

Correspondence should be addressed to Ayushi Verma; ayushiverma09695@gmail.com

Received: 27 January 2026; Revised: 9 February 2026; Accepted: 8 March 2026

ABSTRACT- Manganese oxide nanoparticles (MnO_x NPs), have caught the attention of researchers in recent years, and have emerged as promising nanomaterials in biomedical research due to their unique redox properties, paramagnetic behaviour, and catalytic activity. This review critically analyses reported synthesis strategies, with particular emphasis on plant-mediated green synthesis approaches. Studies show that green-synthesised MnO_x nanoparticles usually range between 5–100 nm. Their shapes can be spherical, tetragonal, rod-like, or sheet-like, depending on the chemical precursors . Plant compounds such as polyphenols and flavonoids help in the formation and stabilization of nanoparticles. The paper also discusses different techniques used to study the size and structure, of nanoparticle including SEM, TEM, XRD, FTIR, and UV–visible spectroscopy. These methods helps to understand the morphology, crystallinity, and surface properties of the nanoparticles. In addition, this review discusses their biomedical uses including MRI, tumor therapy, drug delivery, radiotherapy, magnetic hyperthermia, and antibacterial activity. Although promising results have been reported, challenges related to large-scale production and toxicity studies still need further research.

KEYWORDS- Biomedical applications, Eco-friendly synthesis, Manganese oxide nanoparticles, Nanomedicine, Plant extracts, Wet chemical methods

I. INTRODUCTION

The word “nano” is used to indicate one billionth a meter or 10-9. The term Nanotechnology was coined by Professor Noria Taniguchi of Tokyo Science University in the year 1974 to describe precision manufacturing of materials at the nano meter level. “Nano” is a Greek word synonymous to dwarf meaning extremely small. Nanoparticles are beginning viewed as fundamental building blocks of nanotechnology. [1] However, with its development, the scope of this definition also expanded. Nanoparticles of different sizes have different biomedical purposes. Recently, Whitesides reviewed and interpreted the relationship among nanotechnology, chemistry, and biology.[2] Scientists are interested in nanoparticles because they bridge the gap between bulk materials and atomic and molecular structures. They can be used in a variety of fields [3]. The bulk material is made up of macroparticles with constant characteristics. The number of atoms on the surface grows substantially at the nanoscale, causing the material’s size-dependent characteristics to change [4][5].

A. Synthesis Method

Both top-down and bottom-up methods can be used for preparing MnO_2 nanoparticles as shown in Figure 1**.** Numerous conventional methods have been successfully employed to produce MnO_2 nanomaterials (MDOs) through MnO^{-4} and Mn^{+2} redox reactions. These methods include wet chemical, solvothermal, precipitation, co-precipitation, controlled synthesis, sol–gel, hydrothermal, reflux, pyrolysis, sonochemical, low-temperature solution combustion, self-reacting, microemulsion, photochemical, and forced hydrolysis techniques [6][7]. Common synthesis approaches involve the oxidation of Mn(II) in a basic solution, its oxidation by agents such as oxygen, potassium persulfate, and hydrogen peroxide, or the reduction of permanganate through various means [8][9]. Frequently used reducing agents include nitric acid (HNO_3)[10], sodium hydroxide (NaOH) [11], hydrochloric acid (HCl) [12], and ammonium fluoride (NH_4F) [13]. Furthermore, given the connection between the morphology and size of NPs, it is imperative to devise fabrication techniques that allow optimization of attributes like monodispersity, crystallite size, surface area, crystallinity level, and morphology [8]. It is known that MnO_2 can exist in different structural forms, α-, β-, γ-, δ-, ε- and λ-types and so forth, when the basic structural unit ([MnO_6] octahedron) is linked in different ways. Based on the different [MnO_6] links, MnO_2 can be divided into three categories: the chain-like tunnel structure such as α-, β-, and γ-types, the sheet or layered structure such as δ-MnO_2, and the 3D structure such as λ-type [14]. The properties of MnO_2 are significantly affected by their phases and morphologies; moreover, the operating properties of LIBs also depend on the phase of MnO_2. In this regard, a great effort has been directed toward the preparation of MnO_2 with different phases and various shapes [15]. Generally, MnO_2 nanostructures could be synthesized through the oxidation of Mn^{2+}, reduction of , redox reactions between Mn^{2+} , or direct phase transformation from other manganese oxides. 1D MnO_2 may provide the

possibility of detecting the theoretical operating limits of LIBs, so various 1D MnO_2 nanomaterials have been synthesized [16][17]. Chen et al. have synthesized MnO_2 with different crystal structures (α-, γ-) and morphologies *via* quick precipitation of Mn^{2+} and Mn^{7+} in water isopropanol without using templates or surfactants [18]. In a typical synthesis, $MnCl_2$ (0.18 g) mixed with isopropanol (50 mL) was heated to 83°C in a refluxing process, and then $KMnO_4$ (0.10 g) dissolved in DI water (5 mL) was added to the solution. Finally, MnO_2 nanoneedles were obtained. Singly-crystal nanowires of α- and β-MnO_2 have been prepared in a hydrothermal procedure employing Mn^{2+} with oxidizing reagents such as $(NH_4)_2S_2O_8$ or $KMnO_4$ [15][19].

B. Characterisation

The synthesized manganese oxide nanoparticles can be characterized by employing various techniques for the identification of the structural, morphological, optical, and functional properties of the nanoparticles. The techniques that can be used for the characterization of the synthesized manganese oxide nanoparticles are UV-Visible spectroscopy, X-ray diffraction (XRD), Fourier transform infrared spectroscopy (FTIR), scanning electron microscopy (SEM), transmission electron microscopy (TEM), etc. The UV-Visible spectroscopy technique can be used for the identification of the synthesized nanoparticles. These properties highlight the importance of comprehensive structural and functional characterization to validate the potential applications of manganese oxide nanoparticles in biomedical, catalytic, and environmental fields.

C. Morphological Characterization

- SEM (Scanning Electron Microscope)- SEM makes use of secondary electron imaging to analyze the surface topology and morphology of micron/nanometer-scale minerals [20]. For a comprehensive understanding of the microstructure and mineral components, SEM is usually combined with X-ray techniques to complement the acquired information [21][22][23][24].The infrared spectroscopy method is helpful in identifying chemical species and determining the molecular structure of minerals. This technique has been widely used in mineral characterization [25,26,27,28].

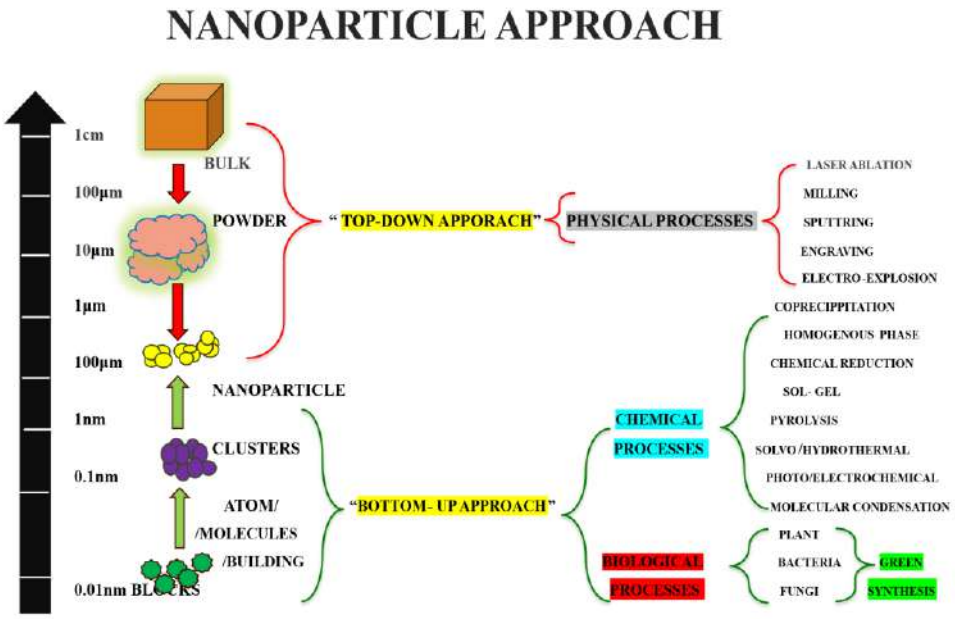

Figure 1: Nanoparticle approaches that are Top-Down and Bottom-Up

- Transmission electron microscopy (TEM)- Transmission electron microscopy (TEM) has long been used in materials science as a powerful analytical tool.[29][30][31][32][33][34] Transmission electron microscopes (TEMs) and their capabilities have benefited enormously from advances in cameras, detectors, sample holders, and computing technologies. However, these advances are hampered by disconnected data streams, limitations of human operation, and cumbersome data analysis [35,36] TEM images, and their associated metadata collected through the MVS software, are organized as an experimental timeline which can be opened and viewed by anyone *via* the free, offline version of the analysis software, Studio (hereafter referred to as the analysis software) [37] TEM images are formed from the interaction between the sample and the electron beam. However, these interactions can also result in negative, inescapable impacts on the sample, such as radiolysis and knock-on damage,[38,39] and require a careful balance between applying a high enough electron dose to generate the image and minimizing the resulting beam damage[40,41]

D. Structural Characterization

XRD- One of the major quantitative analysis methods in mineral analysis is X-ray diffraction (XRD). It correlates the content of minerals with diffraction density, which helps in identifying and quantifying the minerals present in the sample [42,43].For example, XRD can be used to analyze calcite and nahcolite in saline brine [44], evaluate deposits by identifying minerals in phyllite [45], examine

the order degree of dolomite [46], and study the content of calcite and dolomite in carbonate rocks [47]. XRD is a rapid and accurate method for quantitative mineral analysis; however, some mineral compositional structures could lead to errors in analytical results [42]. This method is well performed for identifying NPs both as solitary and multiphase processes. This method is based on incident X-rays being applied to a material and then measuring the X-rays' scattering angles and intensities as they exit from substance [47]. Based on peak intensity, information about crystal structure (atomic positions, temperature factor, or occupancy) as well as texture and quantitative phase analyses can be obtained. Finally, peak shape gives information about sample broadening contributions (micro strains and crystallite size) [48]. However, when samples exhibit highly amorphous properties with varying inter-atomic distance or when nanomaterials are less than few hundred of atoms, resolution and accuracy of XRD may be reduced [49].

E. Surface Chemistry & Functional Group Analysis

FTIR- The oscillatory properties of co-factors and amino acids are investigated using Fourier transform infrared (FTIR) spectroscopy that is delicate to even smallest structure alterations. It is known from studying FTIR spectra that functional groups adhere the surface of biosynthetic non-metals include -C = O-, -NH2, and -SH-groups. [50] For nanomaterial applications, Fourier transform infrared (FTIR) spectroscopy is commonly employed to use the expression of characteristic spectral bands to reveal nanomaterial biomolecule conjugation, e.g. proteins bound to NP surfaces, and to illustrate the conformational states of the bound proteins. [51][52][53][54]

F. Optical Characterization

UV-Visible Spectroscopy

The determination of NP synthesis of various nanoparticles from different methods was analyzed by UV-visible spectroscopy. The production of nanoparticles is clearly indicated by a steady increase in the characteristic peak with increasing reaction time and concentration of biological extracts with salt ions. The UV-vis absorption spectrum of nanosized particles reveals peaks characteristic of the surface plasmon resonance [55]. The feasible range for UV-vis spectroscopy is 200–800 nm range; wavelength underneath 200 nm is considering as vacuum UV while wavelength more than 800 nm is considered infrared. [56]

Chromophores are stimulated when UV-vis light strikes them; this process is known as electron-excitation. On other hand, auxochromes are electron-donating substances that may alter the color of chromophores without changing their own color. A great medium for UV-visible spectroscopy is alcohols and water generally they are transparent and they don't absorb in the UV-vis spectrum [5]. Using UV-vis spectrophotometer, light is passed through a specimen and on other side transmitted light is recorded by detector. Transitions from one band to another, either longer wavelengths (red shifts) or shorter wavelengths (blue shifts), are known as bathochromic shifts and hypochromic. The terms hyperchromic and hypochromic refer to variations in the peak intensity of an absorption band [57]. The transmittance indicates amount of light absorbed at every spectrum, primarily consider greatest peak as λmax. UV-visible spectroscopy is based on electronic transitions of organic molecules that excite electrons from lower energy orbital (highest occupied molecular orbital, or HOMO) to higher energy unoccupied orbital (lowest unoccupied molecular orbital, or LUMO) upon absorption of light [58].

G. Application Of MnO Nanoparticles

Magnetic Hyperthermia- Magnetic hyperthermia is a treatment technique that raises the temperature of a specific tissue above 46°C, which is pretty above the normal physiological temperature (36~37° C), to kill tumor cells. Mn becomes a good option for this improvement approach of MNPs owing to its outstanding biocompatibility. For instances, Haghniaz et al. firstly reported that the dextran-coated lanthanum strontium MnO3-NPs (Dex-LSMO-NPs) had strong ferromagnetism and low Curie temperature and were suitable for hyperthermia applications in vivo. Other than that, CS-coated MnFe2O4 NPs also showed great magnetic properties, especially used in hyperthermia studies for biomedical research. MZF-HA-NPs were developed for synergistic therapy under alternating magnetic field and radiation field. Hyperthermia mediated by dextran-coated La0.7Sr0.3MnO3 nanoparticles: in vivo studies under the controlled magnetic field. Magnetic hyperthermia efficiency is investigated by the specific absorption rate (SAR), which relies on the size, shape, composition, concentration of NPs, and applied magnetic field. A higher SAR value is more favourable as it reduces the dosage and duration of treatment. The necessary therapeutic temperature depends on the size, saturation magnetization (Ms), amplitude, frequency, and time of the applied magnetic field. Generally, ferrites, magnetite, and maghemite are very much employed in hyperthermia studies. Among different ferrites, manganese ferrites are more pertinent for hyperthermia owing to their chemical stability, low inherent toxicity, simple synthesis approach, and exquisite magnetic properties. Besides it is very much suited for MRI and contrast agents. Mn NPs are used as either dopants or combined with other magnetic NPs in hyperthermia studies. Andrade et al.[59][111]

The Table 1 represent a comparative summary of 24 plant-mediated synthesized manganese and manganese oxide nanoparticles, highlighting the plant source, plant part used, elemental form such as (Mn, MnO, MnO_2, Mn_3O_4 etc), particle size, morphology, and their major applications. Most nanoparticles were synthesized using leaf extracts and exhibited sizes within the nanoscale range with predominantly spherical morphology. The synthesized materials demonstrated significant applications in antibacterial activity, dye degradation, electrochemical sensing, environmental remediation, and agricultural enhancement, etc emphasizing the effectiveness of green synthesis approaches.

Table 1: Green synthesis of manganese oxide nanoparticles using plant extracts

S.No.	Plant	Element	Part	Size	Shape	Application
1.	Adalodakam	Mn_3O_4	Leaves	66 nm	Tetragonal Body	Electrochemical utility in catalysis.
2.	Yucca Gloriosa	MnO_2	Leaves	80 nm	Spherical	Degradation of organic dye
3.	Green Tea	MnO	Leaves	20–30 nm	----	Strong antibacterial activity It inhibited the development of E. coli, K. pneumoniae and P. aeruginosa.
4.	Ficus	MnO_2	Leaves	7 to 9 nm	Spherical	It is utilized to remove MG from aqueous solutions effectively.
5.	Eucalyptus Robusta	Mn	Leaves	23.77–28.69 nm	Crystallite	It helps in treatment of corn seeds.
6.	Corymbia Citriodora	Mn	Leaves	14.14-26.18 nm	Spherical	It promotes the growth of the leaf system.
7.	Syzygium Aromaticum	MnO	Powdered Clove	2.5 ± 0.88 n m	-------	Used for the electrochemical detection of PNP, helps in sensing other harmful chemicals.
8.	Ziziphus Abyssini	MnO	Leaves	264 nm	Tetragonal Structure	Antimicrobial activity against E. coli, Staphylococcus aureus, Salmonella typhi, and Shigella.
9.	V. Betonicifolia	MnO_2	Leaves	30–50nm	-------	Antibacterial coatings for medical devices, such as catheters, tubing, sensors, and bandages.
10.	Cinnamomum Verum	Mn	Bark	50 nm-100 nm.	Spherical, Crystalline	Antimicrobial activity against S. aureus and E. coli bacterial Strains.
11.	Sapindus Mukorossi	Mn	Raw	<10 nm	Needle Shape	Ion exchange, catalysis, biosensors, energy storage and adsorption.
12.	(Malpighia Emarginata) Acerola	MnO_2	Leaves	49 ± 13 to 94 ± 47 nm	Crystalline	Anticancer agent against the MCF-7 breast cancer cells.
13.	Plectranthus Amboinicus	MnO_2	Leaves	100 nm.	Spherical	Antifungal activity against A. niger, C. albicans, C. tropicalis and M. campestris
14.	Abutilon Indicum	MnO	Leaf	80 ± 0.5 nm	-----	Photocatalytic against methylene blue, and removal of heavy metal ion (CrVI) by adsorption
15.	Dittrichia Graveolens	MnO	Aerial Parts	38 nm	Spherical	It helps in wastewater treatment, sensors of p-nitrophenol, molecular sieve and catalysis.
16.	Bryophyllum Pinnatum	Alpha – MnO_2	Leaves	4 to 18 nm	Crystalline	It has been used as an electrode material for lithium batteries.
17.	Kalopanax Pictus	MnO_2	Leaves	19.2 nm	Crystalline Nature	Degrade two dyes (congo red and safranin O)
18.	Vernonia Amygdalina	MnO_2	Leaves	20 nm – 22 nm	Crystallite	-------
19.	Cucurbita Pepo	MnO_2	Leaves	5–40nm	Spherical	Antibacterial activity against food- and water-borne bacterial pathogens.
20.	Matricaria Chamomilla	MnO_2	Flower	16.5 nm	Crystallite	Used as catalyst for organic dyes degradation, antibacterial effects against A. oryzae strain RS-2.
21.	Grape Stems and Apple Peels	Alpha - MnO_2	Peels	40-80 nm in diameter.	High-Crystalline	Used for the degradation of aqueous solutions of indigo carmine dye and water purification.

22.	Seeds Of Oat (Avena Sativa L)	MnO_2	Powder	50–-100 nm	Crystallite	Used in the fabrication of modified sensors CPX-PM-MnO2NPs and CTX-PT-CuONPs.
23.	Annona Muricataseed	MnO	Powder	380 nm	Symmetrical	Antimicrobial activity against S. aureus, E. coli, B. subtilis and S. bacillus.
24.	Rose And Lotus Petals	MnO	Powder	21.1 and 26.5 nm	Crystalline	NPs give improved protection from oxidation, corrosion, disintegration, and wear to the composite layer.

II. MRI

MRI was originally known as nuclear magnetic resonance (NMR)139 imaging and belongs to a configuration of NMR, albeit the "nuclear" employed in the acronym was omitted to avoid negative associations with the word [60]. This technique is based on the principles of nuclear magnetic resonance (NMR), and provides a high-resolution image of soft tissues by monitoring the difference in the water molecules relaxation rate (ri =1/Ti) in the tissue [61] where i = 1 or 2 represent the longitudinal relaxation rate (r1) and transverse relaxation rate (r2) respectively, and at the same concentration, higher relaxation rates provide better contrast images. T1-weighted images are often used to assess the anatomical structures at specific sites, while T2-weighted images are often used to monitor the tissue lesions. MRI usually is associated with the problems of prolonged sensitivity and detection time. This can be solved satisfactorily by the use of external drug MRI contrast agents (CAs). When CAs is close to water molecules in the magnetic resonance, it can change the magnetic field environment of water molecules and shorten their longitudinal and transverse relaxation time. These enhances the contrast between the specific targeted tissues and the surrounding tissue, and then enhance the contrast of MRI image [62]. Mn was one of the earliest reported paramagnetic contrast materials for MRI based on its potent positive contrast enhancement. The increased accessibility of Mn centres to adjacent water molecules due to the porous architecture of Mn-NPs greatly enhances the contrast capacity of T1-weighted MRI, thus Mn-NPs appear to be a potential choice for MRI tool exploration. Among them, a variety of Mn oxide NPs, such as MnO, MnO2, Mn3O4, and MnOx NPs have been extensively researched as T1-weighted MRI CAs owing to the short cycle time of Mn2+ chelate and the size-controlled cycle time of colloidal NPs [63]. The manganese in MnO2-based nanomaterials is spatially shielded from water molecules due to its strong coordination with O2 atoms. Therefore, these materials cannot promote the spin−lattice or spin−spin relaxation of protons. However, MnO2 can react with endogenous H2O2 to release Mn2+. Mn2+ is chemically exchanged with protons to increase the T1 signal and achieve high-quality imaging. [64] In contrast, manganese ions (Mn2+), with their paramagnetic properties, offer a safer alternative. They can effectively shorten the T1 relaxation times of water protons, enhancing signal intensity on T1-weighted MRI images without the health risks associated with GBCAs [65]. Mn2+ also impacts T2 relaxation times to a lesser extent, supporting versatile imaging applications [66]. In order to further improve imaging contrast sensitivity, various Mn-doped NPs as T1- or T2-MRI CAs have been developed. [67] Recently, several Mn-derived biomaterials have been proposed as responsive CAs for MRI, including Mn oxides, Mn silicates, and Mn phosphates. Among these materials, MnO2 has garnered considerable attention owing to its established propensity for unstable transformations under biologically relevant pH conditions and redox-modulated states. [68][69][70]

Table 2: Biomedical Application of Mn and MnO Nanostructure

Mn/Mn Oxide Nanoform	**Application**
Mn_3O_4	MRI contrasting agent
MnO	MRI contrasting agent
Mn_3O_4	Dual modality contrasting agent (MRI + fluorescence)
MnO nanocrystals	MRI contrasting agent
Mn	Cancer treatment + drug delivery
MnO_2	Photosensitizer delivery for PTT and PDT
MnO_2	Combined photoand chemotherapy for cancer treatment
MnO_2	Radiosensitizer delivery
MnO_2	Combined photothermal and photodynamic for cancer treatment
MnO	MRI contrasting agent + drug delivery for targeted therapy
MnO_2	Drug delivery for targeted therapy + MRI contrasting agent
MnO_2	Sensitizer (PDT) and drug delivery for targeted therapy +MRI contrasting agent
MnO	Chemodynamic therapy + fluorescent imaging
MnO_2	Starvation/hyperthermia therapy+ MRI and PA contrasting agent

Table 2 shows different manganese precursors used to synthesize nanoparticles and their applications such as MRI imaging, drug delivery, and antibacterial biomaterials.

III. TUMOUR THERAPY [CANCER]

Cancer, a morbid state caused by aberrant cell proliferation, is the second leading cause of death globally.

Cancer caused almost ten million deaths in 2020 on the basis of data released by the World Health Organization (WHO), and unfortunately the incidence of cancer is still rising year by year. [71]

Malignant tumors have always been a serious threat to human health, and its mortality rate ranks second only to cardiovascular diseases. At present, the development of effective and safe anti-tumor drugs with low side effects is the main focusing area in current anti-tumor research and development. Anti-tumor drugs refer to anti-neoplastic drug, which are also known as anti-cancer drugs. Currently, the developed anti-tumor drugs mainly exert anti-tumor effects through the regulation of cell cycle, signal transduction, induction of cell apoptosis, angiogenesis, and the interaction between cells and extracellular matrix, with advantages of high selectivity and low toxicity. The main mechanism of action of these anti-tumor drugs include: (1) killing tumor cells, inhibiting tumor proliferation, promoting cell apoptosis and necrosis; (2) inducing tumor cell differentiation, and irreversibly blocking tumor cell differentiation; (3) blocking tumor invasion and metastasis; (4) Inhibition of tumor angiogenesis, etc [72]. Tumor tissue generally has a leaky vasculature, which allows MnNPs to accumulate at tumor site easily. This is referred to as the enhanced permeation and retention (EPR) effect of Mn-NPs. Incubation of polymeric Mn-NPs in plasma or serum could result in surface enrichment with multifunctional proteins. The targeting ligands of tumor specific biomarkers were conjugated on to Mn-NPs with the opsonization of serum protein to interact with receptors on the tumor cells, allowing for endocytosis and subsequent release of the drug [73]. For instance, folic acid (FA) receptors are highly expressed on the surface of liver cancer cells and breast cancer cells [74][75] so the targeted uptake of tumor cells can be achieved by FA-modified Mn-NPs. MnO2 NPs are easy to prepare and have good stability due to which it has been applied in various fields. The tunnel-like a-MnO2 has been used as an electrocatalyst for oxygen reduction and oxygen evolution in both aqueous and organic electrolytes. [76] Similar to the structures of other 2D materials, MnO2 NSs possess high specific surface areas and a thickness of nanometers to micrometers. Moreover, the redox reactions between MnO2 and glutathione (GSH) in acidic environment have favored their applications in activatable fluorescent biosensors, controlled drug delivery and activable T1-MR imaging. [77][78][79] Once coupled to tumor-targeting ligands such as antibodies, peptides, or small molecules, the nanoparticles target tumor antigens (biomarkers) with great affinity and specificity. [80] Kuo et al. developed gadolinium-Mn-doped magnetism-engineered iron oxide NPs (Gd-MnMEIO-NPs) as a novel contrast agent with enhancement effects in both T1- and T2-weighted MRI of liver with high relaxivity r1 and r2 values. The average hydrodynamic size of Gd-MnMEIO-NPs was 20 nm, and the zeta potential was close to 0 mV, which could effectively avoid their removal from the reticuloendothelial system and prolong their residence time. Gd-MnMEIO-NPs could not only enhance normal liver and living tumor tissues but also improve the visualization of vascular trees. Haemodynamic information from dynamic contrast-enhanced T1-weighted MRI images using Gd-MnMEIO-NPs was helpful to diagnose liver tumors. [81]. It can be used to reveal the detailed information related to tumor, including the location and size of the tumor, before undergoing in vivo photo-chemotherapy to minimize the side effects of treatment, and hence is widely used in the early diagnosis and monitoring of tumors [82]. These advancements give intriguing possibilities for the specific medical specialty of genetic and supramolecular biomarkers routinely utilized for cancer detection and treatment in the molecular profile of individual patients [83].

IV. DRUG DELIVERY

Nanotechnology has revolutionized the field of drug delivery by providing an effective and targeted delivery of drugs, minimizing side effects, and increasing the therapeutic efficacy of drugs. The application of nanotechnology in drug delivery involves the use of nanoparticles that are designed to carry drugs and deliver them to the desired site of action [84]. Nano-drug systems primarily focus on improving the bioavailability of specific tissue delivery, extending injectable medicines' half-life, and orally giving medicinal products. Nano drugs are administered at lower levels, with remarkable improvements in their pharmacological effects and a reduced danger to health and adverse effects.[85][86][87][88][89][90][91]

Additionally, manganese oxide nanoparticles can be utilized to target certain genes in cells, such as cancer cells. Manganese oxide nanoparticles offer special qualities including substantial volume / surface area, multifunctionality, and surface adaptability that have prompted the development and wide adoption of nanotechnology [92][93] Manganese oxides are extensively used for drug delivery applications due to their exclusive properties like biocompatibility, high surface area, redox activity, stimuli– responsive, and tunable surface [94,95,96]. The Mn oxides are used in drug delivery in different forms like MnO2 [97] Mn2O3 [98] Mn3O4 [99] and Mn-based composites [100]. Mn NP is used in different structures like rods [112], 101 spheres [96] wires [102] sheets [103] platelets [104] mesoporous [96] hollow [105] etc. The redox ability of MnO2 makes it more favorable for the triggered drug release by the reversible redox reaction [106] Mn-based NPs are capable of undergoing a Fenton reaction, where Mn ions initiate the decomposition of H2O2 present in the tumor environment and generate oxygen and increase the reactive oxygen species in cancer cells resulting in the activation of oxidative stress which ruins cancer cells [107]. Recently, manganese-based nanomaterials (Mn-based NPs), including nanosheets, hollow structures, nanocages, and nanobubbles, have served as effective reservoirs for drug delivery. Mn can be engineered to produce functional nanomaterials with different valences and functionalities. Mn-based NPs have emerged as promising alternatives owing to their lower toxicity compared to other inorganic nanostructures. They have proven to be efficient systems for drug delivery, owing to their unique physicochemical properties, including ordered mesostructure, uniform porosity, high loading efficacy, and good biocompatibility [108] Marvelous scientific arrangements are being carried out in the form of manufacturing and testing mechanical red blood cell

technologies called respirocytes. Nanorobotics share the potential to deliver 200+ times more oxygen to body tissues as compared to natural red blood cells [109][110] This could make one think about the potential of nanotechnology to be utilized for the diagnosis and treatment of various blood-linked disorders and their cure in the future [110].

Table 3: Manganese-Based Precursors and Their Biomedical Application

S. No	Precursor	Application
1.	Mn (II) acetate Mn (II) stearate	T1 contrast agent Chemotherapy
2.	$KMnO_4$ $MnCl_2$	Glutathione detection Drug delivery
3.	Manganese acetate Manganese nitrate	Image-guided nano-delivery
4.	Manganese (II)	MR/PA/CT imaging siRNA delivery
5.	Mn-containing organic metal alkoxides, esters, etc.	Large surface area-to-mass ratios
6.	$MnCl_2•4H_2O$	MRI contrast agents
7.	Manganese solution	Antibacterial biomaterials

Table 3 presents various manganese oxide nanostructures and their biomedical uses in imaging, targeted drug delivery, and cancer therapies.

V. RADIOTHERAPY

Radiotherapy (RT) is another frequently-used treatment for cancer, which depends on employing high-energy radiation to kill tumor cells. Radiosensitizers can efficiently increase the radiation dose at the cellular level, consequently improving the effect of RT. Mainstream radiosensitizers include alkylating agents that cause DNA damage, inhibitors that block DNA repair, and cell cycle synchronization agents that arrest tumor cells at the more radiosensitive G2/M phase.[111] Thereinto, Mn oxide NPs showed excellent potentials for their unique properties. They could function as not only a good radiosensitizer carrier, but also both a catalase and an oxidant that promoted decomposition of H2O2 into O2 to convert the hypoxic TME, thus enhancing RT efficacy.[112]

Magnetic hyperthermia is a treatment technique that raises the temperature of a specific tissue above 46°C, which is pretty above the normal physiological temperature (36~37° C), to kill tumor cells under the controlled magnetic field. [113] Mn becomes a good option for this improvement approach of MNPs owing to its outstanding biocompatibility. For instances, [114] firstly reported that the dextran-coated lanthanum strontium MnO3-NPs (Dex-LSMO-NPs) had strong ferromagnetism and low Curie temperature and were suitable for hyperthermia applications in vivo [114] Other than that, CS-coated MnFe2O4 NPs also showed great magnetic properties, especially used in hyperthermia studies for biomedical research. [115] MZF-HA-NPs were developed for synergistic therapy under alternating magnetic field and radiation field. [116] Magnetic hyperthermia efficiency is investigated by the specific absorption rate (SAR), which relies on the size, shape, composition, concentration of NPs, and applied magnetic field. A higher SAR value is more favourable as it reduces the dosage and duration of treatment. The necessary therapeutic temperature depends on the size, saturation magnetization (Ms), amplitude, frequency, and time of the applied magnetic field. Generally, ferrites, magnetite, and maghemite are very much employed in hyperthermia studies. Among different ferrites, manganese ferrites are more pertinent for hyperthermia owing to their chemical stability, low inherent toxicity, simple synthesis approach, and exquisite magnetic properties. Besides it is very much suited for MRI and contrast agents. Mn NPs are used as either dopants or combined with other magnetic NPs in hyperthermia studies. Andrade et al. [117]

VI.ANTIBACTERIAL ACTIVITY

Infectious diseases caused by bacteria are the most growing global health problem, infecting millions of people every year [118]. Until now, a number of antibacterial materials, such as antibiotics, quaternary ammonium ion, metal ions, and biocides have been developed to counter the growth of dangerous bacteria [119,120]. However, owing to high cost of the above materials, antibiotic resistance, and complex chemical processing, the provision of alternative antimicrobials is of particular importance [121]. It was found that artificial enzyme mimics are able to function as an antimicrobial against both Gram-positive and Gram-negative bacteria via increasing the transformation of H2O2 into ROS. [122,123]

Bacteria have been found to be favourable candidates (as nanofactories) for the biological synthesis of NPs because they extracellularly produce NPs using the reduction of metal ions to metal particles. Furthermore, the amazing potential of NP production by bacteria may be remarkable due to their faster reproduction rate and easy cultivation [124]. The mechanism of synthesis of all NPs by bacteria remains the same, which typically refers to the synthesis of reductase enzymes by bacteria that contribute to the bio reduction mechanism [126]. Microbial growth can occur in intracellular and extracellular environments, as it reduces magnesium ions to oxide NPs [127]. The extracellular mechanism of biomolecules is based on the release of proteins and enzymes from microorganisms that can reduce and stabilise metal salts. [128]. The use of bacteria-assisted synthesis of nanoparticles was found to be very promising [129]. There are usually two methods regarding the bacteria-assisted synthesis of NPs such as intracellular and extracellular synthesis [130, 12]

VII. CONCLUSION

Manganese oxide nanoparticles are becoming increasingly important due to their excellent properties, particularly in terms of their uses, especially in the medical domain. In this review, different approaches were discussed that are used to synthesize manganese oxide nanoparticles, especially focusing wet chemical methods of green synthesis of Manganese oxide nanoparticles. Among these techniques, green synthesis techniques were found to be an excellent approach, as they do not require any toxic

compounds to be used during the reaction. These advantages of plant-mediated synthesis, apart from making the preparation process easier, also improve the biocompatibility of the synthesized nanoparticles, making them suitable for biomedical applications, for example, antimicrobial activity, drug delivery, and diagnostics. Although there is some achievement reported with regards to nanotechnology and manganese oxide NPs, there is a need for further investigations with regards to manganese oxide NPs for better control, reproducibility, and effects of manganese oxide NPs in the future. There is a promising future with regards to green synthesis of manganese oxide NPs for further nanomedicine investigations.

Table 4: Characteristics and functional Applications of Mn and MnO_2 Nanoparticle

Precursor	Shape	Size	Application
MnO_2	Irregularly spherical,	19.8–63.9 nm	Antibacterial activity (Xanthomonas oryzae pv. oryzae) (At a concentration of 16 μg/mL, the zone of inhibition was 13.2 mm).
$MnSO_4·H_2O$	Spherical	22.32 and 23.42 nm	Micronutrient fertilizers for crop production (Contributed to higher germination rate, longer root system, and increased fresh weight of maize).
$MnCl_2·4H2O$	Spherical	26.98–65.67 nm	Suppressed Fusarium Wilt (*Fusarium oxysporum* f. sp. *niveum* (*Fon*)) in watermelon (The concentration of 100 μg/mL can significantly inhibit the growth of mycelium).
$MnCl_2·4H_2O$	Grained, nanosize, amorphous, round	----	-----
$MnCl_2$	------	60∼200 nm	Highly effective NIR photothermal therapy and dual response magnetic resonance imaging (Bio-MnO_2 NPs exhibited excellent PTT conversion performance, showed ultrasensitive responsiveness to TME, and had high in vivo biocompatibility).
$Mn(CH_3COO)_2·4H_2O$	-------	<20 nm	Antibacterial activity (*Streptococcus muntas*).
$MnCl_2$	-------	----	Removal of biocides, pharmaceuticals, and steroid hormones. (Bio-MnO_x NPs completely removed the steroid hormones estrone and 17-α ethinyl estradiol and removed 26% of diclofenac).
$MnSO_4$	Spherical,	130.2 nm	Degradation of bisphenol A (The photodegradation rate was 66.3%) and antibacterial activity (B. cereus, *E. coli*, *S. enterica*, and *S. aureus*).
$KMnO_4$	Hexagonal and spherical	34.4 nm	------
$KMnO_4$	Spherical	6–28 nm	Photocatalytic activity (rhodamine B, methyl orange, and methylene blue) (The degradation rates were 0.06781, 0.04323, and 0.03831 min^{-1}, respectively, and four cycles could be performed. The whole photocatalytic process followed pseudo-first kinetics).
$MnSO_4·H_2O$	----------	42 nm	As a catalyst for biodiesel production, antibacterial activity (*S. aureus, E. coli, B. subtilis, and K. pneumoniae*), and catalytic reduction of methylene blue (The MB was substantially degraded in less than 1 min).
$MnSO_4$	Spherical	60–80 nm	Photocatalytic reduction of methylene blue and antimicrobial activity (*Micrococcus, S. aureus, E. coli, and Pseudomonas aeruginosa. Aspergillus niger, and Trichoderma viride*).
$MnSO_4$	-------	20–30 nm	Antibacterial activity (*E. coli, Klebsiella pneumoniae* and *Pseudomonas aeruginos*) (MIC was 12.5 U/mL).
$Mn(CH_3COO)_2$		80 nm	Photocatalytic degradation of Acid Orange dye (The degradation rate of the dye is 33% in 20 min).
$Mn(CH_3COO)_2$	Spherical	32 nm	-----
$MnCl_2$	Spherical,	28.7–63.1 nm	Adsorption of aromatic amines (p-Anisidine, p-Toluidine, Aniline, and p-Chloroaniline)
$MnCl_2$	Cubic,	21.6–65.4 nm	Adsorption of aromatic amines (p-Anisidine, p-Toluidine, Aniline, and p-Chloroaniline)
$MnSO_4$	Spherical,	80 ± 0.5 nm	Antibacterial (*E. coli, Bordetella bronchiseptica, S. aureus, and B. subtilis*). (The zone of inhibition was 5, 6, 7, and 9 mm at 10 μg/mL)
$Mn(CH_3COO)_2·4H_2O$	Spherical,	17–35 nm	Antibacterial activity (*S. aureus, Pseudomonas aeruginosa, and*

			Serratiam arcescens)
$KMnO_4$	Spherical,	10–70 nm	Removal of Sb(III) and Sb(V) (The removal rates were 100% and 61.8%, respectively).
$KMnO_4$	Spherical,	10–50 nm	Removal of Sb(III) and Sb(V) (The removal rates were 83.1% and 50.5%, respectively)
$Mn(NO_3)2{\cdot}6H_2O$	------	46.5 nm	Methylene blue degradation and antibacterial activity (*Bacillus subtilis*, *Staphylococcus aureus*, *E. coli*, and *Pseudomonas aeruginosa*)
$Mn(NO_3)2{\cdot}6H_2O$	--------	43.5 nm	Methylene blue degradation and antibacterial activity (*B. subtilis*, *S. aureus*, *E. coli*, and *Pseudomonas aeruginosa*)
$KMnO_4$	Nano spheres	(33 nm) Nano rods (diameter of 4 nm length of 28 nm)	Cytotoxicity and antioxidant activity.
$KMnO_4$	------	40~80 nm	Catalytic degradation of indigo carmine
$KMnO_4$	------	28~70 nm	Catalytic degradation of indigo carmine (The degradation was >80% at 0.025% concentration)
$MnSO_4{\cdot}H_2O$	Spherical,	50.05 nm	Antioxidant and anti-gastric cancer (The IC_{50} against KATOIII is 341 µg/mL).
KMnO4 and MnCl2	Needle	<10 nm	Adsorption of aromatic amines (p-Anisidine, p-Toluidine, Aniline, and p-Chloroaniline).
$Mn(CH_3COO)_2{\cdot}4H_2O$	Rode	50–100 nm	Ultrasensitive modified polymeric sensors
$KMnO_4$	Spherical	7–9 nm	Removal of malachite green from surface water (The maximum adsorption capacity was 277.78–298.328 mg/g following the pseudo-second-order kinetic and Langmuir isotherm models)
$Mn(CH_3COO)_2{\cdot}4H_2O$	-----	41 nm	Photocatalytic degradation of methylene blue.
$Mn(NO_3)_2{\cdot}4H_2O$	-----	28 nm	Remazol turquoise blue G-133 degradation (The degradation rate was 95.3% within 7 h and fits pseudo-second-order kinetics and has an adsorption efficiency of 98%)
$Mn(NO_3)_2{\cdot}4H_2O$	----	32 nm	Adsorption of remazol turquoise blue G-133

Table 4 Presents the precursors, shapes, sizes, and applications of Mn and MnO_2 nanoparticles. These nanoparticles show different shapes and sizes and are used in antibacterial activity, plant disease control, MRI imaging, photothermal therapy, and pollutant degradation.

REFERENCES

[1] Taniguchi N, "On the Basic Concept of Nano-Technology," Proc. Intl. Conf. Prod. Eng., Tokyo, Part II, Japan Society of Precision Engineering, 1974.

[2] Whitesides, G. M., "Nanoscience, nanotechnology, and chemistry," *Small*, vol. 1, no. 2, pp. 172–179. Available from: https://doi.org/10.1002/smll.200400130

[3] Zhang, Y. X., Dong, M., Zhu, S. J., Liu, C. P., and Wen, Z. Q., "Hydrothermally controlled synthesis of 3D dendrite MnOOH nanorods through self-assembly of MnO2 nanoparticles in acid solution," *Physica B Condensed Matter*, vol. 416, pp. 23–28. Available from: https://doi.org/10.1016/j.physb.2013.02.002

[4] Bozon-Verduraz, F., et al., "Nanoparticles of metal and metal oxides: some peculiar synthesis methods, size and shape control, application to catalysts preparation," *Brazilian Journal of Physics*, vol. 39, no. 1a, pp. 134–140. Available from: https://doi.org/10.1590/s0103-97332009000200002

[5] Jassal, V., et al., "Sapindus mukorossi mediated green synthesis of some manganese oxide nanoparticles interaction with aromatic amines," *Applied Physics A*, vol. 122, no. 4. Available from: https://doi.org/10.1007/s00339-016-9777-4

[6] Sukhdev, A., et al., "Synthesis, phase transformation, and morphology of hausmannite Mn3O4 nanoparticles: photocatalytic and antibacterial investigations," *Heliyon*, vol. 6, no. 1, e03245. Available from: https://doi.org/10.1016/j.heliyon.2020.e03245

[7] Yang, S., et al., "Manganese oxide nanocomposite fabricated by a simple solid-state reaction and its ultraviolet photoresponse property," *Chemical Communications*, vol. 47, no. 9, p. 2619. Available from: https://doi.org/10.1039/c0cc04783j

[8] Souri, M., et al., "Procedure optimization for green synthesis of manganese dioxide nanoparticles by Yucca gloriosa leaf extract," *International Nano Letters*, vol. 9, no. 1, pp. 73–81. Available from: https://doi.org/10.1007/s40089-018-0257-z

[9] Chen, H., Tian, W., and Ding, W., "Effect of preparation methods on morphology of active manganese dioxide and adsorption performance," *Adsorption Science & Technology*, vol. 36, no. 3–4, pp. 1100–1111. Available from: https://doi.org/10.1177/0263617417752578

[10] Tang, N., et al., "Facile synthesis of α-MnO2 nanorods for high-performance alkaline batteries," *Journal of Physics and Chemistry of Solids*, vol. 71, no. 3, pp. 258–262. Available from: https://doi.org/10.1016/j.jpcs.2009.11.016

[11] Qu, Q., et al., "Electrochemical performance of MnO2 nanorods," *Journal of Physical Chemistry C*, vol. 113, no.

31, pp. 14020–14027. Available from: https://doi.org/10.1021/jp8113094
[12] Duan, L., et al., "Catalytic degradation of Acid Orange 7," *Journal of Hazardous Materials*, vol. 285, pp. 356–365. Available from: https://doi.org/10.1016/j.jhazmat.2014.12.015
[13] Li, W., et al., "Performance modulation of α-MnO2 nanowires," *Scientific Reports*, vol. 5, p. 8987. Available from: https://doi.org/10.1038/srep08987
[14] Chen, Y., et al., "Synthesis and formation mechanism of α-MnO2," *Journal of Alloys and Compounds*, vol. 490, pp. 331–335. Available from: https://doi.org/10.1016/j.jallcom.2009.10.004
[15] Wang, X., and Li, Y., "Hydrothermal synthesis of MnO2 nanowires," *Journal of the American Chemical Society*, vol. 124, no. 12, pp. 2880–2881. Available from: https://doi.org/10.1021/ja0177105
[16] Kijima, N., et al., "Preparation of α-MnO2," *Journal of Solid State Chemistry*, vol. 159, no. 1, pp. 94–102. Available from: https://doi.org/10.1006/jssc.2001.9136
[17] Huang, M. H., et al., "Room-temperature ultraviolet nanowire nanolasers," *Science*, vol. 292, no. 5523, pp. 1897–1899. Available from: https://doi.org/10.1126/science.1060367
[18] Chen, S., et al., "Shape-controlled synthesis of MnO2," *Crystal Growth & Design*, vol. 9, no. 10, pp. 4356–4361. Available from: https://doi.org/10.1021/cg900223f
[19] Wang, X., and Li, Y., "Rational synthesis of MnO2 nanorods," *Chemical Communications*, no. 7, pp. 764–765.
[20] Li, C., Wang, D., and Kong, L., "Application of machine learning techniques in mineral classification for SEM-EDS images," *Journal of Petroleum Science and Engineering*, vol. 200, p. 108178. Available from: https://doi.org/10.1016/j.petrol.2020.108178
[21] Wen, Y., Cheng, Y., Liu, Z., Liu, C., and Nie, Q., "Application of SEM and EDS for mineral composition of shale gas reservoir," *IOP Conference Series Materials Science and Engineering*, vol. 780, no. 4, p. 042055. Available from: https://doi.org/10.1088/1757-899x/780/4/042055
[22] Nikonow, W., and Rammlmair, D., "Automated mineralogy based on µ-EDXRF microscopy," *Geoscientific Instrumentation, Methods and Data Systems*, vol. 6, no. 2, pp. 429–437. Available from: https://doi.org/10.5194/gi-6-429-2017
[23] Chalouati, S., et al., "Intensified mineral carbonation of natural Canadian silicates," *International Journal of Coal Geology*, vol. 277, p. 104332. Available from: https://doi.org/10.1016/j.coal.2023.104332
[24] Santos, R. M., et al., "CO2 Energy Reactor – Integrated Mineral Carbonation," *Frontiers in Energy Research*, vol. 4. Available from: https://doi.org/10.3389/fenrg.2016.00005
[25] Lammers, K., et al., "CO2 sequestration through mineral carbonation," *Environmental Science & Technology*, vol. 45, no. 24, pp. 10422–10428. Available from: https://doi.org/10.1021/es202571k
[26] Haque, F., Santos, R., and Chiang, Y., "Using nondestructive techniques in mineral carbonation," *Powder Technology*, vol. 357, pp. 134–148. Available from: https://doi.org/10.1016/j.powtec.2019.08.089
[27] Zarandi, A. E., et al., "Nesquehonite as a carbon sink," *Chemical Engineering Journal*, vol. 314, pp. 160–168. Available from: https://doi.org/10.1016/j.cej.2017.01.003
[28] Fantucci, H., et al., "Mineral carbonation as an educational investigation," *Sustainability*, vol. 11, no. 15, p. 4156. Available from: https://doi.org/10.3390/su11154156
[29] Brunelli, M., et al., "Solving larger molecular crystal structures," *Angewandte Chemie International Edition*, vol. 42, no. 18, pp. 2029–2032. Available from: https://doi.org/10.1002/anie.200250607
[30] "Electron Microscopy of Thin Crystals," Internet Archive, 1965. Available from: https://archive.org/details/electronmicrosco0000pbhi
[31] McLaren, A. C., *Transmission Electron Microscopy of Minerals and Rocks*, Cambridge University Press, 2005.
[32] Thomas, J. M., and Midgley, P. A., "High-resolution TEM," *Chemical Communications*, no. 11, pp. 1253–1267. Available from: https://doi.org/10.1039/b315513g
[33] Midgley, P. A., and Dunin-Borkowski, R. E., "Electron tomography and holography," *Nature Materials*, vol. 8, no. 4, pp. 271–280. Available from: https://doi.org/10.1038/nmat2406
[34] Armigliato, A., "Analysis of crystal defects by TEM," *Materials Chemistry*, vol. 4, no. 3, pp. 453–471. Available from: https://doi.org/10.1016/0390-6035(79)90034-8
[35] Thomas, J. M., et al., "The rapidly changing face of electron microscopy," *Chemical Physics Letters*, vol. 631–632, pp. 103–113. Available from: https://doi.org/10.1016/j.cplett.2015.04.048
[36] Spurgeon, S. R., et al., "Towards data-driven TEM," *Nature Materials*, vol. 20, no. 3, pp. 274–279. Available from: https://doi.org/10.1038/s41563-020-00833-z
[37] Egerton, R., Li, P., and Malac, M., "Radiation damage in TEM and SEM," *Micron*, vol. 35, no. 6, pp. 399–409. Available from: https://doi.org/10.1016/j.micron.2004.02.0034
[38] Grubb, D. T., "Radiation damage and electron microscopy," *Journal of Materials Science*, vol. 9, no. 10, pp. 1715–1736. Available from: https://doi.org/10.1007/bf00540772
[39] Buban, J. P., et al., "Low-dose STEM," *Journal of Electron Microscopy*, vol. 59, no. 2, pp. 103–112. Available from: https://doi.org/10.1093/jmicro/dfp052
[40] Chen, Q., et al., "Imaging beam-sensitive materials," *Advanced Materials*, vol. 32, no. 16, e1907619. Available from: https://doi.org/10.1002/adma.201907619
[41] Ali, A., Chiang, Y. W., and Santos, R. M., "X-ray diffraction techniques for mineral characterization," *Minerals*, vol. 12, no. 2, p. 205. Available from: https://doi.org/10.3390/min12020205
[42] Klug, H. P., and Alexander, L. E., *X-Ray Diffraction Procedures*, Wiley-Interscience, 1974.
[43] Ali, A., et al., "Production of sodium bicarbonate with CO2 co-utilization," *Crystals*, vol. 13, no. 3, p. 470. Available from: https://doi.org/10.3390/cryst13030470
[44] Chi, G. C., et al., "Application of X-ray powder diffractometer," *Geological Resources*, vol. 22, pp. 409–414, 2013.
[45] Zhang, X. H., "Controlling factors of dolomite," *Lithology and Reservoirs*, vol. 21, pp. 50–55, 2009.
[46] Trindade, M., et al., "Mineralogical transformations of clays," *Applied Clay Science*, vol. 42, no. 3–4, pp. 345–355. Available from: https://doi.org/10.1016/j.clay.2008.02.008
[47] Prasad, A. S., "Green synthesis of Mn oxide," *Materials Science in Semiconductor Processing*, vol. 71, pp. 342–347. Available from: https://doi.org/10.1016/j.mssp.2017.08.020
[48] Hoseinpour, V., et al., "Green synthesis and photocatalytic activity," *Micro & Nano Letters*, vol. 13, no. 11, pp. 1560–1563. Available from: https://doi.org/10.1049/mnl.2018.5008
[49] Saod, W. M., et al., "Biosynthesis and antibacterial activity," *Biotechnology Reports*, vol. 34, e00729. Available from: https://doi.org/10.1016/j.btre.2022.e00729
[50] Hasan, I. M. A., et al., "Ficus-mediated green synthesis," *Environmental Science and Pollution Research*, vol. 30, no. 10, pp. 28144–28161. Available from: https://doi.org/10.1007/s11356-022-24199-8
[51] Gonçalves, J. P. Z., et al., "Green synthesis for agricultural applications," *Colloids and Surfaces A*, vol. 636, p.

128180. Available from: https://doi.org/10.1016/j.colsurfa.2021.128180
[52] Kumar, V., Singh, K., Panwar, S., and Mehta, S. K., "Green synthesis of manganese oxide nanoparticles for electrochemical sensing," *International Nano Letters*, vol. 7, no. 2, pp. 123–131. Available from: https://doi.org/10.1007/s40089-017-0205-3
[53] Yelwa, J., "Green synthesis and characterization of manganese oxide nanoparticles using Ziziphus Abyssinia," vol. 16, p. 8. Available from: https://www.researchgate.net/publication/366485853
[54] Lu, H., et al., "Biogenic synthesis of MnO2 nanoparticles using leaf extract," *Frontiers in Microbiology*, vol. 12. Available from: https://doi.org/10.3389/fmicb.2021.761084
[55] Kamran, U., et al., "Biogenic synthesis and photocatalytic activity of manganese nanoparticles," *Journal of Molecular Structure*, vol. 1179, pp. 532–539. Available from: https://doi.org/10.1016/j.molstruc.2018.11.006
[56] Revathi, N., et al., "Green synthesis of MnO2 nanoparticles and antimicrobial activity," *Inorganic Chemistry Communications*, vol. 154, p. 110935. Available from: https://doi.org/10.1016/j.inoche.2023.110935
[57] Khan, S. A., et al., "Green synthesis of MnO nanoparticles using plant extract," *Biomolecules*, vol. 10, no. 5, p. 785. Available from: https://doi.org/10.3390/biom10050785
[58] Levy, S. B., and Marshall, B., "Antibacterial resistance worldwide," *Nature Medicine*, vol. 10, S122–S129. Available from: https://doi.org/10.1038/nm1145
[59] Zhao, Z., et al., "Octapod iron oxide nanoparticles for MRI," *Nature Communications*, vol. 4. Available from: https://doi.org/10.1038/ncomms3266
[60] Liu, Z., et al., "Theranostic MnO2 nanosheets for tumor microenvironment," *Biomaterials*, vol. 155, pp. 54–63. Available from: https://doi.org/10.1016/j.biomaterials.2017.11.015
[61] Small, W., et al., "MRI contrast agent study," *Academic Radiology*, vol. 5, pp. S147–S150. Available from: https://doi.org/10.1016/s1076-6332(98)80087-1
[62] Rief, M., et al., "Manganese-based oral contrast agent for MRI," *Investigative Radiology*, vol. 45, no. 9, pp. 565–571. Available from: https://doi.org/10.1097/rli.0b013e3181e9e120
[63] Siegel, R. L., et al., "Cancer statistics 2021," *CA: A Cancer Journal for Clinicians*, vol. 71, no. 1, pp. 7–33. Available from: https://doi.org/10.3322/caac.21654
[64] Zhao, H., et al., "Metal–organic frameworks as nanocarriers," *ACS Applied Materials & Interfaces*, vol. 13, no. 5, pp. 6034–6042. Available from: https://doi.org/10.1021/acsami.0c21006
[65] Moghimi, S., and Szebeni, J., "Stealth liposomes and nanoparticles," *Progress in Lipid Research*, vol. 42, no. 6, pp. 463–478. Available from: https://doi.org/10.1016/s0163-7827(03)00033-x
[66] Law, S., et al., "Folic acid-modified nanoparticles for anticancer activity," *Artificial Cells Nanomedicine and Biotechnology*, vol. 48, no. 1, pp. 542–559. Available from: https://doi.org/10.1080/21691401.2020.1725025
[67] Gong, T., et al., "Magnetic graphene oxide nanocomposites for liver cancer," *Journal of Inorganic Biochemistry*, vol. 223, p. 111558. Available from: https://doi.org/10.1016/j.jinorgbio.2021.111558
[68] Benbow, E. M., et al., "Oxygen reduction properties of manganese oxide electrocatalysts," *Journal of Physical Chemistry C*, vol. 115, no. 44, pp. 22009–22017. Available from: https://doi.org/10.1021/jp205544
[69] Lin, L., et al., "MnO2-based nanoagent for chemodynamic therapy," *Angewandte Chemie International Edition*, vol. 57, no. 18, pp. 4902–4906. Available from: https://doi.org/10.1002/anie.201712027
[70] Xu, Y., et al., "Carbon dots–MnO2 platform for glutathione detection," *Nanoscale*, vol. 8, no. 27, pp. 13414–13421. Available from: https://doi.org/10.1039/c6nr03129c
[71] Hasan-Abad, A. M., et al., "Functional deimmunization of interferon beta," *Iranian Journal of Allergy Asthma and Immunology*. Available from: https://doi.org/10.18502/ijaai.v18i4.1421
[72] Kuo, Y., et al., "Gadolinium-labeled nanoparticles for MRI," *PLoS ONE*, vol. 11, no. 2, e0148695. Available from: https://doi.org/10.1371/journal.pone.0148695
[73] Paul, G., et al., "MnII-containing nanoparticles as MRI contrast agents," *Chemical Communications*, vol. 50, no. 51, pp. 6740–6743. Available from: https://doi.org/10.1039/c4cc01251h
[74] Cuillel, M., et al., "CuO nanoparticles interference in hepatocytes," *Nanoscale*, vol. 6, no. 3, pp. 1707–1715. Available from: https://doi.org/10.1039/c3nr05041f
[75] Sahu, T., et al., "Nanotechnology-based drug delivery systems," *Journal of Drug Delivery Science and Technology*, vol. 63, p. 102487. Available from: https://doi.org/10.1016/j.jddst.2021.102487
[76] *Global Health Journal*, KeAi Publishing. Available from: https://www.keaipublishing.com/en/journals/global-health-journal/
[77] Li, J., et al., "Cellular labeling and drug release using quantum dots," *Science China Chemistry*, vol. 57, no. 6, pp. 833–841. Available from: https://doi.org/10.1007/s11426-014-5092-0
[78] Parani, S., et al., "Biopolymer encapsulation of CdTe quantum dots," *Advanced Materials Research*, vol. 584, pp. 258–262. Available from: https://doi.org/10.4028/www.scientific.net/amr.584.258
[79] Abdelhamid, H. N., et al., "CdS-modified chitosan quantum dots," *Carbohydrate Polymers*, vol. 214, pp. 90–99. Available from: https://doi.org/10.1016/j.carbpol.2019.03.024
[80] Chen, T., et al., "Core–shell nanocarriers for tumor-targeted drug delivery," *Carbohydrate Polymers*, vol. 92, no. 2, pp. 1124–1132. Available from: https://doi.org/10.1016/j.carbpol.2012.10.022
[81] Su, X., et al., "Graphene quantum dot nanoprobe for drug delivery," *Biosensors and Bioelectronics*, vol. 92, pp. 489–495. Available from: https://doi.org/10.1016/j.bios.2016.10.076
[82] Wu, P., et al., "Methotrexate-conjugated quantum dots," *Materials Letters*, vol. 128, pp. 412–416. Available from: https://doi.org/10.1016/j.matlet.2014.04.167
[83] Katz, E., and Willner, I., "Nanoparticle–biomolecule hybrid systems," *Angewandte Chemie International Edition*, vol. 43, no. 45, pp. 6042–6108. Available from: https://doi.org/10.1002/anie.200400651
[84] Kong, R., et al., "Aptamer-conjugated nanomaterials," *Science China Chemistry*, vol. 54, no. 8, pp. 1218–1226. Available from: https://doi.org/10.1007/s11426-011-4336-5
[85] Haque, S., et al., "Manganese-based nanoparticles for biomedical applications," *Nanoscale*, vol. 13, no. 39, pp. 16405–16426. Available from: https://doi.org/10.1039/d1nr04964j
[86] Shin, J., et al., "Hollow manganese oxide nanoparticles," *Angewandte Chemie International Edition*, vol. 48, no. 2, pp. 321–324. Available from: https://doi.org/10.1002/anie.200802323
[87] Liu, X., and Rong, P., "Recent advances of manganese-based hybrid nanomaterials for cancer precision medicine," *Frontiers in Oncology*, vol. 11. Available from: https://doi.org/10.3389/fonc.2021.707618
[88] Yadav, P., Bhaduri, A., and Thakur, A., "Manganese oxide nanoparticles: structure, synthesis and applications," *ChemBioEng Reviews*, vol. 10, no. 4, pp. 510–528. Available from: https://doi.org/10.1002/cben.202200056

[89] Chen, J., et al., "Functionalized MnO2 nanosheets for biosensing," *Nanoscale Horizons*, vol. 4, no. 2, pp. 321–338. Available from: https://doi.org/10.1039/c8nh00274f
[90] Zhang, Z., and Ji, Y., "Nanostructured manganese dioxide for anticancer applications," *Nanoscale*, vol. 12, no. 35, pp. 17982–18003. Available from: https://doi.org/10.1039/d0nr04067c
[91] Yasun, E., et al., "Hollow micro and nanostructures for therapeutic applications," *Journal of Drug Delivery Science and Technology*, vol. 60, p. 102094. Available from: https://doi.org/10.1016/j.jddst.2020.102094
[92] Wen, J., Yang, K., and Sun, S., "MnO2-based nanosystems for cancer therapy," *Chemical Communications*, vol. 56, no. 52, pp. 7065–7079. Available from: https://doi.org/10.1039/d0cc02782k
[93] Yang, G., Ji, J., and Liu, Z., "Multifunctional MnO2 nanoparticles for tumor therapy," *Wiley Interdisciplinary Reviews Nanomedicine and Nanobiotechnology*, vol. 13, no. 6. Available from: https://doi.org/10.1002/wnan.1720
[94] Chen, Y., Cong, H., Shen, Y., and Yu, B., "Biomedical application of MnO2 nanomaterials," *Nanotechnology*, vol. 31, no. 20, p. 202001. Available from: https://doi.org/10.1088/1361-6528/ab6fe1
[95] Enrico, C., "Nanotechnology-based drug delivery of natural compounds," *Studies in Natural Products Chemistry*, pp. 91–123. Available from: https://doi.org/10.1016/b978-0-444-64185-4.00003-4
[96] Suhail, M., et al., "Micro and nanorobot-based drug delivery," *Journal of Drug Targeting*, vol. 30, no. 4, pp. 349–358. Available from: https://doi.org/10.1080/1061186x.2021.1999962
[97] Gong, L., et al., "Application of radiosensitizers in cancer radiotherapy," *International Journal of Nanomedicine*, vol. 16, pp. 1083–1102. Available from: https://doi.org/10.2147/ijn.s290438
[98] Wang, S., et al., "MSOT/CT/MR imaging-guided radiotherapy using MnO2 nanoparticles," *Nanoscale*, vol. 11, no. 13, pp. 6270–6284. Available from: https://doi.org/10.1039/c9nr00918c
[99] Farzin, A., et al., "Magnetic nanoparticles in cancer therapy," *Advanced Healthcare Materials*, vol. 9, no. 9. Available from: https://doi.org/10.1002/adhm.201901058
[100] Haghniaz, R., et al., "Hyperthermia mediated by nanoparticles," *International Journal of Nanomedicine*, p. 1779. Available from: https://doi.org/10.2147/ijn.s104617
[101] Islam, K., et al., "Manganese ferrite nanoparticles for MRI," *Nanomaterials*, vol. 10, no. 11, p. 2297. Available from: https://doi.org/10.3390/nano10112297
[102] Wang, H., et al., "Theranostic platform for dual imaging-guided therapy," *Nanoscale*, vol. 12, no. 8, pp. 5139–5150. Available from: https://doi.org/10.1039/c9nr10039c
[103] Andrade, R. G. D., et al., "Synthesis and cytotoxicity of ferrite nanoparticles," *Pharmaceutics*, vol. 14, no. 12, p. 2694. Available from: https://doi.org/10.3390/pharmaceutics14122694
[104] Choi, K., et al., "Multifunctional magnetic particles for bacteria killing," *Chemical Communications*, vol. 48, no. 38, p. 4591. Available from: https://doi.org/10.1039/c2cc17766h
[105] Paladini, F., et al., "Metal-based antibacterial substrates," *Biomacromolecules*, vol. 16, no. 7, pp. 1873–1885. Available from: https://doi.org/10.1021/acs.biomac.5b00773
[106] Cocco, A. R., et al., "Antibacterial monomers in dental systems," *Dental Materials*, vol. 31, no. 11, pp. 1345–1362. Available from: https://doi.org/10.1016/j.dental.2015.08.155
[107] Levy, S. B., and Marshall, B., "Antibacterial resistance worldwide," *Nature Medicine*, vol. 10, S122–S129. Available from: https://doi.org/10.1038/nm1145
[108] Natalio, F., et al., "Vanadium pentoxide nanoparticles and biofilm inhibition," *Nature Nanotechnology*, vol. 7, no. 8, pp. 530–535. Available from: https://doi.org/10.1038/nnano.2012.91
[109] Gao, L., et al., "Ferromagnetic nanoparticles with enzyme-like activity," *Nanoscale*, vol. 6, no. 5, pp. 2588–2593. Available from: https://doi.org/10.1039/c3nr05422e
[110] Saravanan, A., et al., "Biosynthesis of metal nanoparticles," *Chemosphere*, vol. 264, p. 128580. Available from: https://doi.org/10.1016/j.chemosphere.2020.128580
[111] Gahlawat, G., and Choudhury, A. R., "Biosynthesis of nanoparticles by microbes," *RSC Advances*, vol. 9, no. 23, pp. 12944–12967. Available from: https://doi.org/10.1039/c8ra10483b
[112] Jacob, J. M., et al., "Microbial synthesis of semiconductor nanoparticles," *Microbial Biotechnology*, vol. 9, no. 1, pp. 11–21. Available from: https://doi.org/10.1111/1751-7915.12297
[113] Banik, A., et al., "Molecular mechanisms of microbial nanoparticle synthesis," *Advances in Environmental Microbiology*, pp. 135–166. Available from: https://doi.org/10.1007/978-3-030-97185-4_6
[114] Dikshit, P. K., et al., "Green synthesis of metallic nanoparticles," *Catalysts*, vol. 11, no. 8, p. 902. Available from: https://doi.org/10.3390/catal11080902
[115] Qamar, S. U. R., and Ahmad, J. N., "Nanoparticles biosynthesis using biological systems," *Journal of Molecular Liquids*, vol. 334, p. 116040. Available from: https://doi.org/10.1016/j.molliq.2021.116040
[116] "Inorganic Chemistry Communications," Elsevier. Available from: https://www.sciencedirect.com/journal/inorganic-chemistry-communications
[117] Nejati, M., et al., "Green methods for MgO nanomaterials," *Inorganic Chemistry Communications*, vol. 136, p. 109107. Available from: https://doi.org/10.1016/j.inoche.2021.109107
[118] Chan, W. C. W., and Nie, S., "Quantum dot bioconjugates," *Science*, vol. 281, no. 5385, pp. 2016–2018. Available from: https://doi.org/10.1126/science.281.5385.2016
[119] Vaseashta, A., and Dimova-Malinovska, D., "Nanostructured devices and sensors," *Science and Technology of Advanced Materials*, vol. 6, no. 3–4, pp. 312–318. Available from: https://doi.org/10.1016/j.stam.2005.02.018
[120] Langer, R., "Drugs on target," *Science*, vol. 293, no. 5527, pp. 58–59. Available from: https://doi.org/10.1126/science.1063273
[121] Roy, K., et al., "Oral gene delivery using nanoparticles," *Nature Medicine*, vol. 5, no. 4, pp. 387–391. Available from: https://doi.org/10.1038/7385
[122] Sachlos, E., et al., "Collagen scaffolds reinforced with nanocrystals," *Tissue Engineering*, vol. 12, no. 9, pp. 2479–2487. Available from: https://doi.org/10.1089/ten.2006.12.2479
[123] Farokhzad, O. C., et al., "Targeted nanoparticle-aptamer bioconjugates," *Proceedings of the National Academy of Sciences*, vol. 103, no. 16, pp. 6315–6320. Available from: https://doi.org/10.1073/pnas.0601755103
[124] Stoimenov, P. K., et al., "Metal oxide nanoparticles as bactericidal agents," *Langmuir*, vol. 18, no. 17, pp. 6679–6686. Available from: https://doi.org/10.1021/la0202374
[125] Sondi, I., and Salopek-Sondi, B., "Silver nanoparticles as antimicrobial agent," *Journal of Colloid and Interface Science*, vol. 275, no. 1, pp. 177–182. Available from: https://doi.org/10.1016/j.jcis.2004.02.012
[126] Panáček, A., et al., "Silver colloid nanoparticles," *Journal of Physical Chemistry B*, vol. 110, no. 33, pp. 16248–16253. Available from: https://doi.org/10.1021/jp063826h

[127] Morones, J. R., et al., "Bactericidal effect of silver nanoparticles," *Nanotechnology*, vol. 16, no. 10, pp. 2346–2353. Available from: https://doi.org/10.1088/0957-4484/16/10/059

[128] Baker, C., et al., "Synthesis and antibacterial properties of silver nanoparticles," *Journal of Nanoscience and Nanotechnology*, vol. 5, no. 2, pp. 244–249. Available from: https://doi.org/10.1166/jnn.2005.034

[129] Singh, A., and Amiji, M. M., "Application of nanotechnology in medical diagnosis," *Current Opinion in Biotechnology*, vol. 74, pp. 241–246. Available from: https://doi.org/10.1016/j.copbio.2021.12.011

[130] Mansouri, A., Gattolliat, C., and Asselah, T., "Mitochondrial dysfunction in chronic liver diseases," *Gastroenterology*, vol. 155, no. 3, pp. 629–647. Available from: https://doi.org/10.1053/j.gastro.2018.06.083

ABOUT THE AUTHOR

Ayushi Verma done Bachelor of Science (Life Sciences) University of Delhi, India College: Kalindi College Year of Completion: 2025 Major Subjects: Molecular Biology, Biochemistry, Microbiology, Immunology

Achievements: Selected as Research Intern at ICMR-NICBR, a premier national biomedical research institute under ICMR.

Presented poster on Computation Analysis of Parkin Gene and Their Role in the Parkinson Disease

Intern in the Research project entitled "Green Synthesis of Silver Nanoparticle from Leaf Extract of Ocimum sanctum And Their Antibacterial Properties"